Recombinant reporter phage rTUN1::*nLuc* enables rapid detection and real-time antibiotic susceptibility testing of *Klebsiella pneumoniae* K64 strains

Peter Braun[1§]*, Rene Raab[1§], Joachim J Bugert[1], Simone Eckstein[1]

[1] Bundeswehr Institute of Microbiology, Munich, Germany

[§]authors contributed equally
*Correspondence: peter3braun@bundeswehr.org

Abstract

The emergence of multi drug resistant (MDR) *Klebsiella pneumoniae* (*Kp*) strains constitutes an enormous threat to global health as MDR associated treatment failure causes high mortality rates in nosocomial infections. Rapid pathogen detection and antibiotic resistance screening is therefore crucial for successful therapy and thus, patient survival. Reporter phage-based diagnostics offer a way to speed up pathogen identification and resistance testing, as integration of reporter genes into highly specific phages allow real-time detection of phage replication and thus, living host cells. *Kp* specific phages use the host's capsule, a major virulence factor of *Kp*, as receptor for adsorption. To date, 80 different *Kp* capsule types (K-serotypes) have been described with predominant capsule types varying between different countries and continents. Therefore, reporter phages need to be customized according to the locally prevailing variants. Recently, we described the autographivirus vB_KpP_TUN1 (TUN1), which specifically infects *Kp* K64 strains, the most predominant capsule type at the military hospital in Tunis (MHT) that is also associated with high mortality rates. In this work, we developed the highly specific recombinant reporter phage rTUN1::*nLuc*, which produces Nanoluciferase (nLuc) upon host infection and thus, enables rapid detection of *Kp* K64 cells in clinical matrices such as blood and urine. At the same time, rTUN1::*nLuc* allows for rapid antibiotic susceptibility testing and therefore identification of suitable antibiotic treatment in less than 3 hours.

Introduction

The ESKAPEE bacteria (*Enterococcus faecium*, *Staphylococcus aureus*, *Klebsiella pneumoniae*, *Acinetobacter baumanni*, *Pseudomonas aeruginosa*, *Escherichia coli* and *Enterobacter* species) are responsible for the majority of nosocomial infections and typically possess multi-drug resistance (MDR). Among these, the opportunistic pathogen *K. pneumoniae* (*Kp*) poses a particular threat for public health. Ubiquitously occurring as a commensal, *Kp* can be found among gastro-intestinal microbiota, in the respiratory tract and on the skin. As a facultative pathogen, *Kp* can cause a variety of severe nosocomial diseases such as pneumonia, sepsis, wound- and urinary tract infections (UTIs). In recent years, the number of community-acquired cases of *Kp*-caused pneumonia and meningitis has dramatically increased (Herridge et al., 2020). Together with the emergence of acquired MDR against broad-spectrum antibiotics (ABs) and the natural resistances of the bacterium, treatment of *Kp*

infections has become a global healthcare challenge (Babini & Livermore, 2000; Knothe et al., 1983; Prestinaci et al., 2015).

Infections with carbapenem-resistant *Kp* are associated with serious symptoms and high mortality rates (Patel et al., 2008; Schwaber et al., 2008). Therefore, rapid diagnosis of the infection as well as detection of resistance markers are crucial for patient survival. Classical approaches to identify carbapenem-resistant *Kp* rely on bacterial cell culture with subsequent biochemical profiling and therefore provide results only after a few days. While nucleic acid based tools such as diagnostic real-time PCR or loop-mediated isothermal amplification (LAMP) enable fast and specific detection of the pathogen, the established assays mainly target carbapenem-resistance genes and therefore cannot distinguish between living cells and DNA residues present in the sample (Hartman et al., 2009; Kurupati et al., 2004; Nakano et al., 2015).

Diagnostic bacteriophages (phages) represent a promising alternative approach. In addition to their therapeutic potential, phages are suited for the identification of bacteria due to the viruses' high specificity. Phage sensitivity assays have been in practice for centuries for a variety of pathogens such as *Bacillus anthracis* (Turnbull et al., 2008) or *Yersinia pestis* (Garcia et al., 2008). Such techniques include antibody-based detection of phages using ELISA (Stewart et al., 2013) or detection of amplified phage DNA (Anany et al., 2018). Another option is to exploit the bacteriolytic activity of phages and detect released cellular components such as ATP (Blasco et al., 1998). The most promising methodology, however, is the use of reporter phages, which either have a reporter molecule directly attached to the virion surface or produced during phage replication (Goodridge et al., 1999; Hennes & Simon, 1995; Meile et al., 2020).

While most phages of gram negative bacteria utilize surface structures such as lipopolysaccharides (LPS), teichoic acids or proteins as host receptors for adsorption (Nobrega et al., 2018), the specificity of *Kp* phages is mostly determined by the different *Kp* capsule polysaccharides (CPS). CPS represent a major virulence factor of *Kp* as the thick layer protects the bacterial cell from phagocytosis and prevents complement binding during host response. In addition, the CPS forms a physical barrier towards ABs as it hampers diffusion into the bacterial cell (Domenico et al., 1994; Merino et al., 1992; Shon et al., 2013). To date, about 80 different *Kp* capsule serotypes (K-types) have been described (Pan et al., 2015). Since *Kp* specific phages are usually capable of infecting only one or a few capsule types, the selection of a suitable reporter phage is crucial for reliable diagnostics. As predominant capsule types vary from region to region, reporter phages need to be customized according to the locally prevailing variant. In Tunisia, e.g., the majority of nosocomial infections at the Military Hospital of Instructions in Tunis (MHT) are caused by a *Kp* strain featuring capsule type 64 (K64). These *Kp* K64

70 infections are associated with high mortality rates, especially among intensive care patients (Eckstein
71 et al., 2021).
72 In this study, we genetically engineered the recently identified *Kp* K64-specific phage vB_KpP_TUN1
73 (TUN1), and constructed a recombinant TUN1 reporter phage (rTUN1::*nLuc*) for the rapid detection of
74 *Kp* K64 strains in bacterial cell culture or directly from clinically relevant matrices as well as for
75 conducting real-time antibiotic susceptibility testing.
76

77 ## Material and Methods

78 **Bacterial growth**

79 All *K. pneumoniae* and *E. coli* strains were cultivated in LB-broth [10% NaCl (w/v), 10% peptone (w/v),
80 5% yeast extract (w/v)] at 37° C under constant shaking.

81 ***In vitro* DNA-Assembly of synthetic phage genomes**

82 For isolation of genomic DNA (gDNA) of phages Master-Pure™ Complete DNA and RNA Purification Kit
83 (Lucigen, Wisconsin, USA) was used according to the supplier's protocol. Prior to assemble the
84 synthetic TUN1 WT genome, TUN1 WT gDNA was used as PCR template to amplify five fragments. This
85 was achieved by using the primer pairs TUN1 F1 + R1 (= Fragment 1), TUN1 F2 + R2 (= Fragment 2),
86 TUN1 F3 + R3 (= Fragment 3), TUN1 F4 + R4 (= Fragment 4) and TUN1 F5 + R5 (= Fragment 5). Primers
87 were designed to generate 15-25 bp overlaps between adjacent fragments to ensure efficient
88 assembly. The circular approach was done in the same way, with the difference of replacing Fragment
89 1 and Fragment 5 by Fragment 5_1, amplified using the primers TUN1 F5 + R1 (Supplementary Figure
90 S1A).

91 If not stated differently, the four TUN1 fragments of the circular approach described above were used
92 for all further TUN1 DNA assemblies.

93 In order to generate the deletion strain TUN1 Δhpgc1, Fragment 5_1 was replaced by Fragment 5_1
94 gp1 (using the primer pair TUN1 F5 + gp1 R) and Fragment 2 by Fragment 2 gp5 (primers TUN1 gp5 F
95 and 2R). TUN1 Δhpgc2 was achieved by using Fragment 5_1 gp6 (primers TUN1 F5 and gp6 R) and
96 Fragment 2 gp9 (primer pair TUN1 gp9 F + R2). For TUN1 Δhpgc3 construction, the primer TUN1 gp9 R
97 and gp12 F were used instead of primer TUN1 2R and 3F, respectively, resulting in the new amplicons
98 Fragment 2 gp9_2 and Fragment 3 gp12 (Supplementary Figure S1D). In each case, TUN1 WT gDNA
99 was used as a PCR template.

100 To generate the triple mutant TUN1 Δhpgc123, Fragment 3 and Fragment 4 were amplified from TUN1
101 WT gDNA using the primer pairs mentioned above. Amplification of modified Fragment 1 was achieved
102 by using the primers TUN1 F5 and gp6 R and gDNA of TUN1 Δhpgc1 as a PCR template. Furthermore,

103 Fragment 2 was amplified from TUN1 Δhpgc2 gDNA by using the primer pair TUN1 gp9 F + R2
104 (Supplementary Figure S1E).

105 To construct rTUN1::*nLuc* either TUN1 WT or TUN1 Δ*gp7-8* gDNA was used as a PCR template. In both
106 cases, four fragments (F 5_1, 2, 3 and 4) were amplified using the primers TUN1 fwd5 + TUN1 rev1,
107 TUN1 fwd2+ rev2, TUN1 fwd3 + TUN1 MajCap rev, TUN1 MinCap fwd + TUN1 rev4. *nLuc* was amplified
108 from pNL2.1 (Promega, Walldorf, Germany) using the primer pair nLuc IGR Cap fwd/rev.

109 For all approaches DNA-Assembly was conducted using the NEBuilder DNA-Assembly Master Mix (New
110 England Biolabs, Ipswich, USA) according to the manufacturer's protocol. Oligonucleotide sequences
111 are listed in Supplementary Table S1. Primer design and *in-silico* cloning was carried out using Geneious
112 Prime (Version 2021.1.1, Biomatters New Zealand)

113 **Phage rebooting**

114 Phage assembly and rebooting was achieved in a non-replicative host by transforming chemically
115 competent *E. coli* 10-beta cells (New England Biolabs) with 5 µl of the assembly mix according to the
116 protocol provided by the manufacturer. After transformation 950 µl of LB medium were added and
117 the cells grown for 2 hours at 37° C with horizontal shaking at 120 rpm. Subsequently, the cells were
118 harvested for 5 min at 3,000 x g and the supernatant, containing rebooted phages, stored at 4° C until
119 further use.

120 **Plaque-Assay**

121 To check for functionality of (recombinant) TUN1 a fresh culture of *Kp* was grown to OD_{600}= 0.4-0.6
122 and then 350 µl of the culture were mixed with 2.5 ml hand-warm soft-agar [LB + 0.6 % Agar (w/v)]
123 together with 100 µl of phage stock/ transformation supernatant. Then, the mixture was evenly
124 distributed on a LB-agar plate and, after solidification, the plates were incubated at 37° C for 16 h. The
125 next day, plaque forming units (PFUs) were calculated and plaque morphology analyzed.

126 **Bacterial growth**

127 To determine the bacteriolytic activity of TUN1 phages on *Kp* strains, bacterial growth was measured
128 comparing samples with and without phages. For this purpose, 100 µl of the respective *Kp* culture (10^7
129 CFUs/ml) were mixed with either 100 µl of TUN1 phage stock ($1x10^3$ PFUs/ml) or 100 µl of LB medium
130 as a control in a 96-well plate with clear bottom. Plates were incubated at 37° C with shaking and
131 bacterial growth (OD_{600nm}) was measured every 30 min.

132 **rTUN1::*nLuc* functionality**

133 To measure luciferase activity on plaque containing LB-agar plates, 5 µl of the diluted (1:50, in PBS)
134 NanoLuc® luciferase substrate 2-furyl methyl-deoxy-coelenterazine (Furimazine; Promega) were
135 dropped onto the respective plaques. After incubation at RT for 3 min, the plates were analyzed for
136 luminescence signals using a ChemiDoc Imaging System and Image Lab 6.0.1 software (Bio-Rad
137 Laboratories Inc., Hercules, USA). Exposure time was set to 5 sec. The obtained luminescence signals
138 were then merged with an image of the plate for identification of plaques featuring luciferase activity.

139 To analyze luminescence in liquid culture medium over time, 100 µl of a fresh *Kp* culture ($1x10^7$ – 1
140 CFUs/ml) mixed with 100 µl of rTUN1::*nLuc* stock ($1x10^3$ PFUs/ml) were transferred into a cavity of a
141 96-well plate and supplemented with 2 µl of substrate. The plate was then incubated at 37° C under
142 continuous shaking (420 rpm) using a Varioskan Lux plate reader (Thermo Fisher Scientific, Waltham,
143 USA). Bacterial growth (OD_{600nm}) and luminescence (exposure time: 100 ms) were measured every 30
144 min for up to 16 h.

145 **Clinical matrices**

146 For rTUN1::*nLuc* based *Kp* detection in clinically relevant matrices, the reporter phage was added to
147 *Kp*-spiked urine and blood samples. Fresh urine was sterile filtered (0.22 µm luer lock syringe filter,
148 Merck Millipore, Cork, Ireland) spiked with the TUN1 host *Kp* 7984 (final conc. $1x10^7$ CFUs/ml).
149 Subsequently, bacterial growth and luminescence were measured in a plate reader every 30 min for 7
150 h at 37° C as described above.

151 To test the clinical matrix blood, 5 ml defibrinated sheep blood, spiked with the *Kp* 7984 (final conc.
152 $1x10^7$ CFUs/ml) was used. Prior to measurements, the serum was collected as described elsewhere
153 (Matsui et al., 2019). Briefly, the 5 ml spiked blood were injected into a 50 S-Monovette® (Sarstedt,
154 Nuernbrecht, Germany) and centrifuged at 2,000 x g for 15 min. The serum containing the bacterial
155 cells was then transferred into a fresh tube and centrifuged again. After discarding the supernatant,
156 the bacteria were resuspended to the original volume using LB medium. Subsequently, bacterial
157 growth and luminescence with and without the presence of rTUN1::*nLuc* was measured as described
158 above.

159 **Data analysis**

160 Sequence data was analyzed using Geneious Prime (Version 2021.1.1). All Varioskan data was analyzed
161 using the SkanIt 6.1 RE for Microplate Readers RE Software (Version 6.1.0.51) and GraphPad Prism
162 (Version 8.4.3).

163

164 Results

165 **Successful rebooting of TUN1 from synthetic phage genomes requires circularized DNA**

166 Generation of TUN1 (an Autographivirus featuring a 41 kb sized genome) reporter phages was aimed
167 to be achieved by synthetic biology driven genetic engineering. As a proof of concept, the technical
168 feasibility of *in vitro* assembly and phage rebooting had to be demonstrated prior to construction of
169 reporter phages. For this, the TUN1 wildtype (WT) DNA was PCR amplified as five or four overlapping
170 fragments and assembled *in vitro* generating linear or circularized synthetic phage genomes,
171 respectively. Recombinant phage TUN1 was successfully rebooted by transforming the non-replicative
172 host *E. coli* NEB Stable with circularized synthetic constructs while transformation of linear constructs
173 did not result in any rebooted phages (Supplementary Figure S2). In a next step, we aimed at
174 integrating the NanoLuc® luciferase gene (*nLuc*) fused to a ribosomal binding site (RBS) into the
175 synthetic circular construct. As insertion site for the RBS-*nLuc* construct, the intergenic region between
176 the major (*gp38*) and the minor (*gp39*) capsid genes was selected (Figure 1), as it qualifies for efficient
177 transcription of the reporter due to the strong *cps* promoter regulating this operon (Loessner et al.,
178 1996a). After *in vitro* DNA-assembly and phage rebooting, however, no plaques were observed on the
179 *Kp* K64 strain 7984 indicating that no functional recombinant reporter phage particles had been
180 generated. Thus, while recombinant phage can be assembled from DNA fragments and rebooted, a
181 recombinant phage with the additional reporter gene *nLuc* cannot.

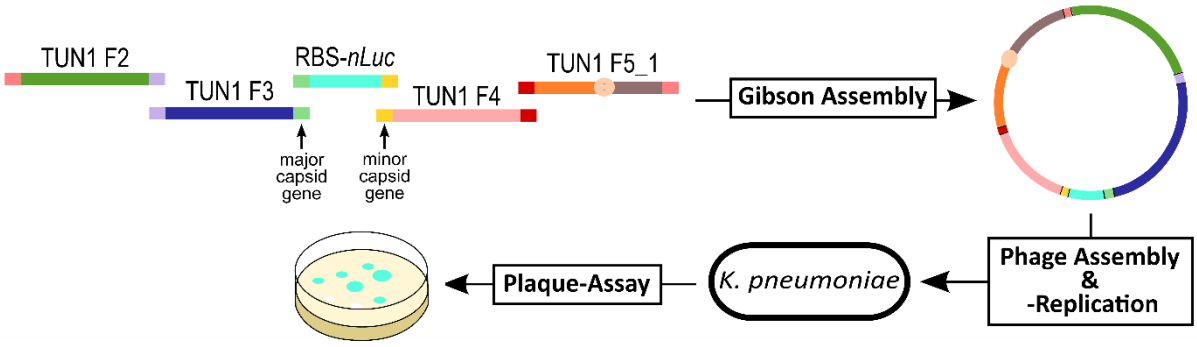

182

183 **Figure 1. Schematic overview of TUN1 repoter phage construction.** For construction of a TUN1 reporter phage all synthetic
184 DNA fragments were amplified with overlapping ends between consecutive segments (depicted in matching colors). After *in*
185 *vitro* DNA assembly the circular DNA was used to transform *E. coli* cells in which the recombinant phages were rebooted.
186 Cells were lysed to release virions from the phage insusceptible host and the lysate used to infect *Kp*. Next, recombinant
187 phage was *in vivo* amplified in its host *Kp* forming plaques on a lawn in the bacteria. Functional reporter phages were screened
188 by measuring plaque luminescence after addition of luminogenic substrate.

189 **Genome reduction of TUN1 enables insertion of *nLuc*-reporter**

190 One possible explanation for unsuccessful reporter integration was that the capacity of DNA
191 encapsulation in the nascent virions is already reached with the size of the WT genome of TUN1. To
192 address this challenge, we next aimed to reduce the TUN1 WT genome to provide space for insertion
193 of the *nLuc* construct. As TUN1 comprises multiple ORFs encoding proteins of unknown function

194 (Eckstein et al., 2021), these hypothetical genes (hpg) without any known function represent ideal
195 candidates for targeted gene deletion. We decided to eliminate the operons *gp2-4*, *gp7-8* and *gp10-*
196 *11* (Figure 2A) as these clusters were predicted to be regulated by single promoters, respectively. For
197 this, we used the same method as described for TUN1 WT *in vitro* assembly above but excluded the
198 selected hpg clusters (hpgc) during fragment amplification (Supplementary Figure S1), resulting in
199 TUN1 Δhpgc1, Δhpgc2 and Δhpgc3 featuring genome reductions by 518 bp, 529 bp and 738 bp,
200 respectively (Figure 2B). As all hpgc deletion variants resulted in functional phages, a triple deletion
201 strain (TUN1 Δhpgc123) was generated by using the single-cluster deletion mutants as PCR-templates
202 for subsequent synthetic phage genome rebooting. This resulted in a reduced genome size by 1,785
203 bp (Figure 2B). Analysis of the recombinant phages for their lytic activities against their host *Kp* 7984
204 in growth experiments, yielded no difference between TUN1 WT and the deletion variants (Figure 2C).
205 While the plaque sizes of TUN1 Δhpgc1 and Δhpgc2 on *Kp* 7984 were similar to that of TUN1 WT, those
206 of the deletion variants TUN1 Δhpgc3 and Δhpgc123 were slightly decreased. As the size of genome
207 reduction in TUN1 Δhpgc2 (529 bp) perfectly matched the size of the *nLuc* construct (526 bp) this
208 variant was used for reporter gene insertion in the next step.

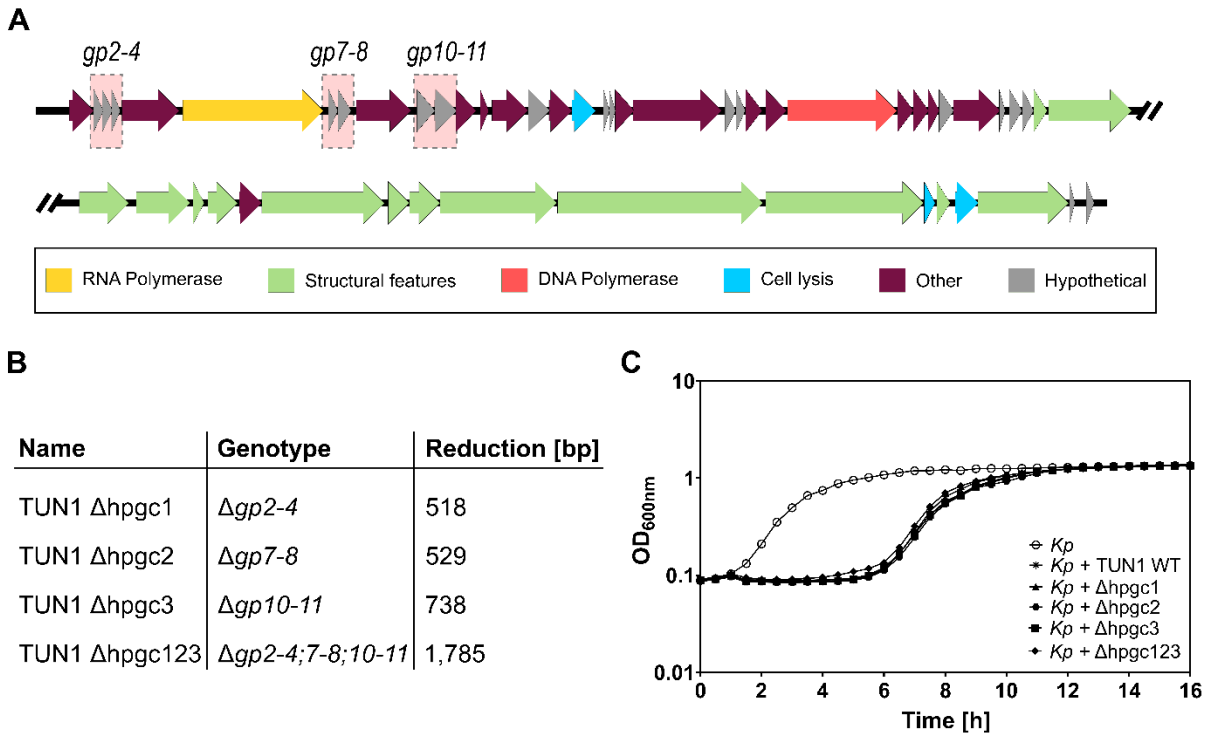

Name	Genotype	Reduction [bp]
TUN1 Δhpgc1	Δ*gp2-4*	518
TUN1 Δhpgc2	Δ*gp7-8*	529
TUN1 Δhpgc3	Δ*gp10-11*	738
TUN1 Δhpgc123	Δ*gp2-4;7-8;10-11*	1,785

209

210 **Figure 2**. **Characteristics of TUN1 deletion variants. A)** Schematic illustration of TUN1 genome. Hypothetical gene clusters
211 *gp2-4*, *gp7-8* and *gp10-11* are shaded in red. **B)** TUN1 deletion variants and their respective genome reduction. **C)** Growth
212 curves of *Kp* 7984 without phage (○), in the presence of TUN1 WT (∗), Δhpgc1 (▲), Δhpgc2 (●), Δhpgc3 (■) or Δhpgc123 (◆).

213 Using the genome-reduced TUN1 Δhpgc2 as a template, we were able to insert the *nLuc* construct and
214 thus to generate phage rTUN1::*nLuc.* Just like TUN1 WT and TUN1 Δhpgc2*,* rTUN1::*nLuc* also formed
215 distinct clear plaques surrounded by translucent halos when tested in plaque assay on *Kp* 7984. To

216 ascertain the functionality of the luciferase reporter, rTUN1::*nLuc* plaques were spot-covered with
217 furimazin, the substrate of NanoLuc® luciferase, and subsequently analyzed for luminescence. Indeed,
218 all plaques emitted light upon addition of furimazin (Figure 3) and therefore, rTUN1::*nLuc* can be used
219 for luminescence-based detection of *Kp* K64.

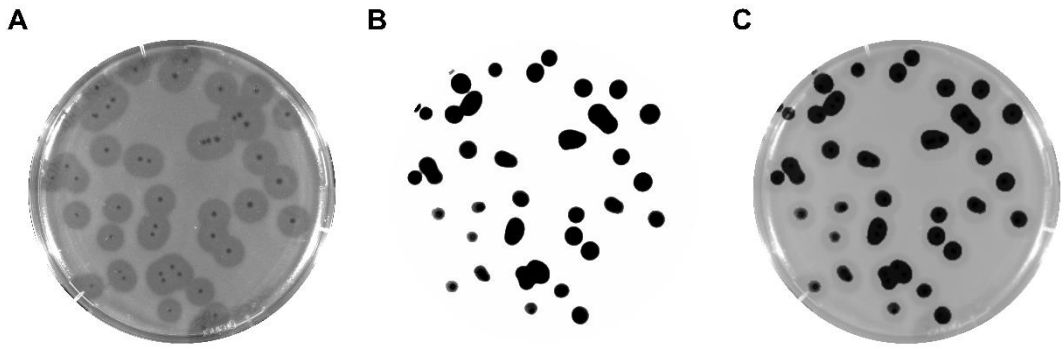

220

221 **Figure 3. Nanoluciferase activity of rTUN1::*nLuc* plaques. A**) Photographic image of a typical plaque assay agar plate with
222 recombinant reporter phage rTUN1::*nLuc* on *Kp* 7984 cells. **B**) Luminescent signal emitted from the agar plate (A) after
223 addition of luminogenic substrate (exposure time: 5 sec). **C**) Merged image of A and B.

224 **rTUN1::*nLuc* enables highly sensitive *Kp* K64 detection**

225 Plaque assays depend on bacterial growth on agar plates and are thus too time consuming for *Kp*
226 detection in clinical diagnostics. Therefore, the next step was to test the applicability of the reporter
227 phage rTUN1::*nLuc* for rapid luminescence-based *Kp* detection in liquid culture. For this, a liquid
228 culture of *Kp* 7984 ($1x10^6$ CFUs per well) was infected with $1x10^2$ PFUs (per well) of the reporter phage
229 and bacterial growth and luminescence were measured over time. We observed an immediate strong
230 increase of luminescence reaching a maximum of 10^8 relative light units (RLUs) after only 2 h of
231 incubation. This increase in luminescence correlated well with the start of impaired bacterial growth
232 compared to the control containing only *Kp* without rTUN1*::nLuc* (Figure 4A). Most probably caused
233 by autodegradation of the substrate, some luminescent background noise was also detected for *Kp*
234 7984 without phage. Therefore, the threshold for positive luminescence results was set to RLUs ≥ 10^3.
235 When different rTUN1::*nLuc* titers were tested, we observed high baseline luminescence (≥ 10^3 RLUs)
236 for phage titers greater than $1x10^3$ PFUs/well, even in phage-only control samples. This is most
237 probably due to carryover of NanoLuc® luciferase during preparation of rTUN1::*nLuc* phage stocks. An
238 initial titer of $1x10^2$ PFUs/well, on the other hand qualified as ideal phage concentration as the baseline
239 was comparable to the one produced by the no-phage control (Supplementary Figure S3).

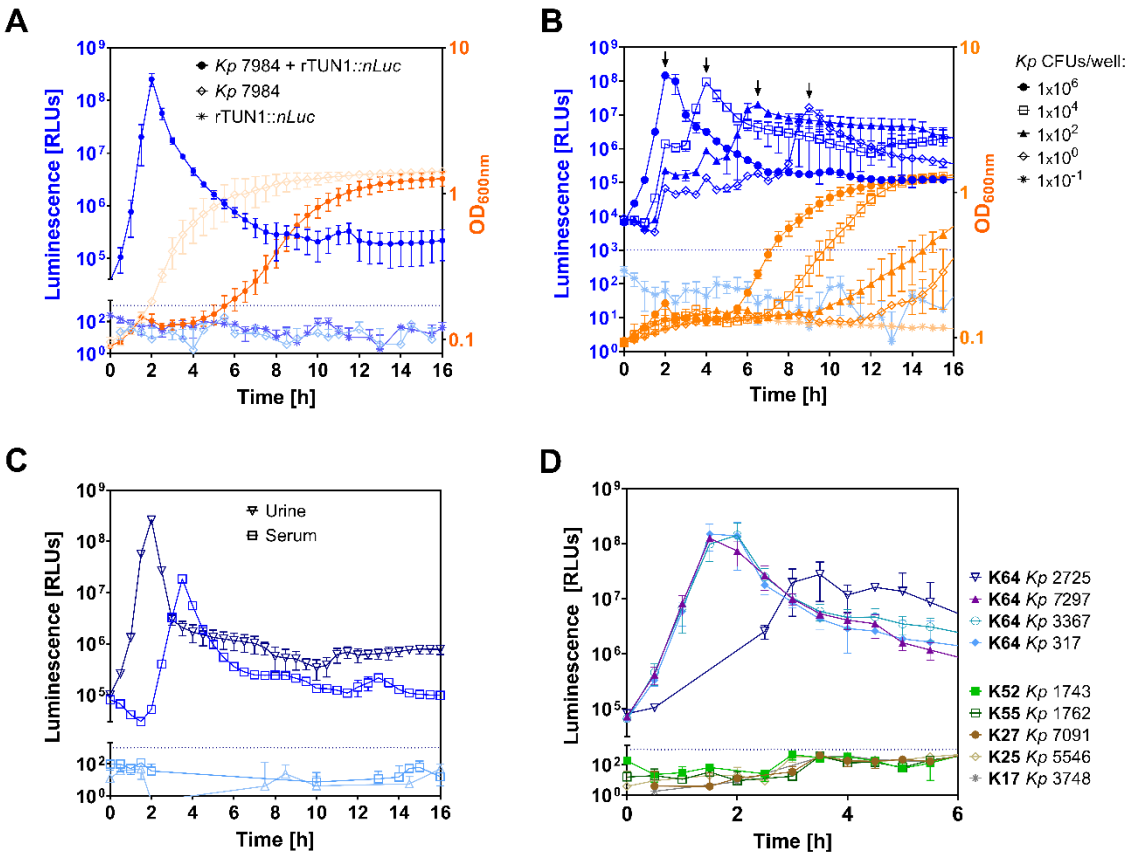

Figure 4. Luminescence based detection of *Kp* K64 using rTUN1::*nLuc*. A) Luminescence (blue) and bacterial growth (orange) measured for *Kp* 7984 ($1x10^6$ CFUs/well with (●) and without rTUN1::*nLuc* (◇) as well as solely rTUN1::*nLuc* (✱) over time. **B)** Luminescence (blue) and bacterial growth (orange) of different *Kp* 7984 concentrations per well (●: $1x10^6$ CFUs; □: $1x10^4$ CFUs; ▲: $1x10^2$ CFUs; ◇: $1x10^0$ CFU; ✱: $1x10^{-1}$ CFU) in the presence of rTUN1::*nLuc*. Black arrows (⬇) indicate the luminescence peaks generated by rTUN1::*nLuc* on respective bacterial culture. **C)** Luminescence for *Kp* 7984 + rTUN1::*nLuc* (dark blue) and without phage (light blue) in urine (▽) and serum (□). **D)** Luminescence of rTUN1::*nLuc* with *Kp* of different K-types (K64, K52, K55, K27, K25 and K17). For every experiment, an initial titer of 10^2 PFUs per well of the respective phage was used. Dotted blue line = threshold of 10^3 RLUs.

To investigate the sensitivity and thus the detection limit of the rTUN1::*nLuc* based reporter phage assay, a dilution series of *Kp* 7984 ($1x10^6$ – 0.1 CFUs per well) was tested using a starting concentration of $1x10^2$ PFUs/well of the reporter phage. Both the increase in detectable bacterial growth as well as the luminescence signal peak was delayed by 2-4 h with every dilution step. (Figure 4B). From this data a standard curve was generated which can be used to easily determine *Kp* concentrations based on the time of luminescence peak (Supplementary Figure S4). The results revealed that as few as one initial cell per well was sufficient to yield a luminescent signal with its peak at 10^7 RLUs after approx. 9 hours. However, some of these wells with 10^0 *Kp* cells turned out negative (in luminescence and optical density) most probably because random distribution of single cells results in empty wells in some cases.

260 **_Kp_ K64 cells can be detected directly in clinical matrices using rTUN1::_nLuc_**

261 _Kp_ can cause severe infections with fatal clinical outcomes, including UTI or sepsis. Therefore, urine
262 and blood represent relevant clinical matrices for _Kp_ diagnostics. Using our reporter phage
263 rTUN1::_nLuc_ on both _Kp_-spiked ($1x10^6$ CFUs/well) urine and blood samples, respectively, distinct
264 luminescence peaks could be measured. Conversely, no matrix associated increase in background
265 luminescence was detected (Figure 4C). While the results for spiked urine samples were almost
266 identical to those measured in spiked growth medium, the luminescence peaks retrieved from spiked
267 blood samples appeared to be time-shifted by 2 h now correlating with the results of an initial _Kp_
268 concentration of $1x10^4$ CFUs/well. This can most easily be explained by a loss of 10^2 bacteria per ml
269 during serum collection from spiked blood.

270 **rTUN1::_nLuc_ is highly specific for _Kp_ K64 strains**

271 Recently, we described that TUN1 WT exclusively infects _Kp_ K64 strains (Eckstein et al., 2021). In order
272 to verify the host specificity of rTUN1::_nLuc_, we analyzed the luminescence development in liquid
273 culture testing four additional _Kp_ K64 strains and five _Kp_ strains with other K-types (K55, K52, K27, K25
274 and K17) in the presence of the reporter phage. Positive signals (> 10^3 RLU) were obtained only from
275 samples containing _Kp_ K64 strains indicating that rTUN1::_nLuc_ features the same specificity for _Kp_ K64
276 strains as the WT phage (Figure 4D).

277 **rTUN1::_nLuc_ enables rapid, real-time antibiotic susceptibility testing of _Kp_**

278 The main challenge for treatment of _Kp_ infections is the increasing number of MDR _Kp_ strains. For
279 instance, _Kp_ 7984, the strain used in this work, has already been shown to be resistant to the first-line
280 AB ertapenem (Kollenda et al., 2019). Testing of antibiotic susceptibilities of _Kp_ strains derived from
281 patient samples is therefore crucial to ensure successful therapy. However, these tests require a pure
282 culture of the infection-causing strain and often contain long incubation steps. To accelerate this
283 process of selecting the adequate ABs for an efficient therapy, we tested whether rTUN1::_nLuc_ is also
284 suitable for the real-time, rapid AB susceptibility testing. For this, we used the experimental settings
285 of the luminescent reporter phage assay (10^6 CFUs/well _Kp_ 7984 + 10^2 PFUs/well rTUN1::_nLuc,_ shown
286 in Fig. 4A) and supplemented the growth medium with various ABs of different classes using their
287 minimal inhibitory concentration (MIC) at breakpoints determined for _Enterobacteriaceae_
288 (Supplementary Table S1). We observed no increase in reporter phage associated luminescence in the
289 presence of gentamicin (Gent), chloramphenicol (Cmp), imipenem (Imp), meropenem (Mer) and
290 amoxicillin/clavulanic acid (Amc) (Figure 5A). In contrast, we detected a strong luminescence increase
291 resulting in a distinct peak after 2 hours, comparable to that of the _Kp_ 7984 + rTUN1::_nLuc_-control
292 without ABs, when levofloxacin (Lev), ceftazidim (Caz), streptomycin (Str), tigecyclin (Tgc+),
293 ciprofloxacin (Cip) and trimethoprim/sulfamethoxazol (T/S) had been added (Figure 5B). Growth
294 experiments of _Kp_ 7984 (without phage) in the presence of ABs further revealed that Gent, Cmp, Imp,

295 Mer and Amc inhibited bacterial growth whereas *Kp* 7984 growth was not affected by the presence of
296 Caz, Str, Tgc+, Cip and T/S (Supplementary Figure S5). Thus, *Kp* 7984 can be considered sensitive to
297 Gent, Cmp, Imp, Mer and Amc and resistant to Caz, Str, Tgc+, Cip and T/S. In contrast to time consuming
298 classical growth experiments and MIC testing, our luminescent reporter phage assay using rTUN1::*nLuc*
299 not only enables rapid and sensitive detection of *Kp* K64 strains directly from clinical samples, but also
300 allows for simultaneous, real-time antibiotic susceptibility testing within just a few hours.

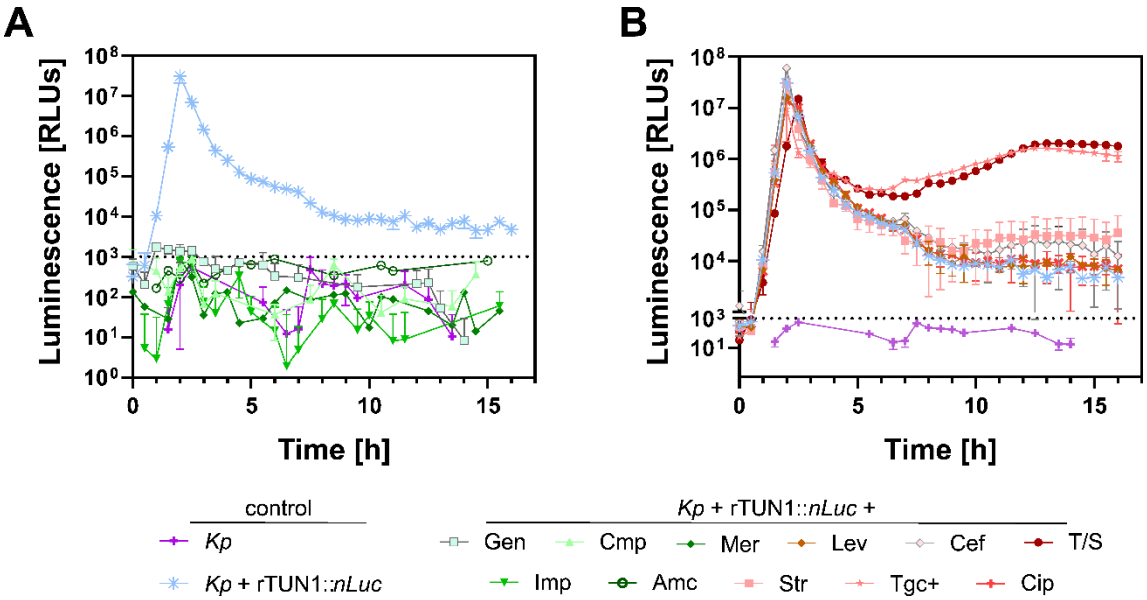

301

302 **Figure 5. Antibiotic susceptibility testing of *Kp* using rTUN1::*nLuc*.** Luminescence measurements of wells containing
303 rTUN1::*nLuc*-infected *Kp* 7984 ($1x10^6$ CFUs + $1x10^2$ PFUs per well) in the presence of different antibiotics. *Kp* without phage
304 (purple) and *Kp* + rTUN1::*nLuc* in pure LB (blue) served as controls **(A)** Despite the positive control no luminescence peak was
305 detected for wells containing *Kp* + rTUN1::*nLuc* in gentamicin (Gen), chloramphenicol (Cmp), imipenem (Imp), meropenem
306 (Mer) or amoxicillin/ clavulanic (Amc). **(B)** Distinct luminescence peaks were generated in samples containing *Kp* +
307 rTUN1::*nLuc* with levofloxacin (Lev), ceftazidime (Caz), streptomycin (Str), tigecyclin (Tgc+), ciprofloxacin (Cip) or
308 trimethoprim/ sulfamethoxazole (T/S). Error bars represent three independent biological replicates.
309

310

311 ## Discussion

312 The enormous increase of antibiotic resistances in bacteria has been estimated to lead to an excess
313 mortality of 10 million persons per year by 2050, mostly caused by nosocomial infections (Alebachew
314 Woldu, 2016; Borer et al., 2009). The multiple antibiotic resistance crisis constitutes a tremendous
315 threat to global health and has been declared a global health emergency (Toner et al., 2015) - a view
316 supported by WHO. Rapid pathogen detection and antibiotic resistance screening allows non-empirical
317 therapy and saves lives. Established methods for *Kp* detection are time consuming and necessitate
318 empirical antibiotic therapy in urgent cases (Davenport et al., 2017) with more unfavorable outcomes.
319 Here, we demonstrated that reporter phage-based diagnostics could be a promising alternative, as
320 integration of reporter genes into highly specific phages enable real-time detection of phage
321 replication and thus, living host cells. Besides fluorescent proteins (Jain et al., 2012) and hydrolyzing

322 enzymes such as β-galactosidase (Chen et al., 2017; Chen et al., 2017)), luciferases can be used as
323 reporters (Hinkley et al., 2018; Loessner et al., 1996b; Meile, Sarbach, et al., 2020; Nguyen et al., 2017).

324 Since the discovery of luciferin-luciferase systems almost a century ago (McElroy & Ballentine, 1944),
325 several luciferase enzymes have become available to researchers. The latest commercially available
326 luciferase is the NanoLuc® enzyme (nLuc) which has several advantages compared to other luciferase
327 systems: It features a relatively small size of only 19.1 kDa (compared to e.g. the Renilla or Firefly
328 luciferase with 36 kDa or 61 kDa, respectively), fast substrate turnover rates - which leads to generation
329 of a high-intensity luminescent signal - and exhibits high stability under various buffer conditions
330 (England et al., 2016; Hall et al., 2012). Therefore, nLuc was selected as reporter candidate for this
331 study.

332 Inserting reporter genes, or any additional nucleotide sequence, into phage genomes can be
333 challenging. As DNA length and capsid size and thus internal pressure in the capsid correlate,
334 (Nurmemmedov et al., 2007) the DNA encapsulation capacity of most phages is limited. Hence,
335 integration of additional genes can negatively affect capsid stability and therefore lead to severe
336 impairments in phage assembly or replication (Grayson et al., 2006; Nurmemmedov et al., 2012). DNA
337 packaging of tailed phages relies on the recognition of specific sequences (*cos*- or *pac*-sites) by the
338 terminase protein followed by DNA cleavage. Depending on the phage type, this cleavage can be either
339 sequence-specific (e.g. T7 or λ) or nonspecific (e.g. P22 or SPP1). For the latter, the cleavage does not
340 occur at the end of the phage genome (so-called termination cleavage) but follows the mechanism of
341 headful packaging where nonspecific DNA cleavage by TerL (terminase large subunit) is induced by
342 increased capsid pressure. As a result, phages using the headful system often tolerate a genome size
343 of up to 110% while the others will not (Casjens & Gilcrease, 2009). Since TerL initiates DNA packaging
344 and cleavage, phylogenetic analysis of the *terl* gene can be used to predict a phage's DNA packaging
345 system. For TUN1, results of this analysis suggested that the phage belongs to the "T7-like group with
346 directed terminal repeats" and not to the "P22-like headful group". Therefore, the fact that our *nLuc*
347 reporter construct could not be inserted into the full-length TUN1 WT genome can most likely be
348 explained by its sequence-specific DNA packaging mechanism in combination with a genome size that
349 has already reached the maximum capsid capacity.

350 It has already been described, that insertion of additional genetic information into the genomes of
351 other *Podoviridiae* or *Autographiviridae* requires preceded genome reduction in order to overcome
352 the problem of limited capsid capacity (Kim et al., 2014; Pires et al., 2021). In this work, we were able
353 to minimize the TUN1 genome by up to 4.3 % (TUN1 Δhpgc123) and, at the same time, demonstrated
354 that the hypothetical genes *gp2-4*, *gp7-8* and *gp10-11* are not essential for a successful lytic cycle of
355 TUN1. Using the genome-reduced TUN1 Δhpgc2 as a template, insertion of the RBS-*nLuc* reporter

356 construct was successful. The resulting, luminescent reporter phage, rTUN1::*nLuc,* enabled specific and
357 sensitive detection of *Kp* K64 cells exhibiting a limit of detection (LOD) of only CFU per well.

358 To our knowledge, there are only two other *Kp*-specific nLuc-based reporter phages, Mcoc and 8M7,
359 that specifically detect *Kp* K21 cells with a comparably low LOD of only 10 CFUs/well and 100 bacteria
360 per 100 mg feces, respectively (Zelcbuch et al., 2021). Other *nLuc*-based reporter phage assays
361 exhibited similar sensitivity. For instance, Pulkkinen et al constructed a T7-*nLuc* phage*,* which was able
362 to detect 47 *E. coli* cells per well (Pulkkinen et al., 2019). Further, ΦV10nluc phage-based *E. coli*
363 detection exhibited an even lower LOD of only 5 CFUs/well. These assays, however, were not tested
364 on clinically relevant matrices. In contrast, our novel rTUN1::*nLuc* based reporter phage assay enables
365 rapid detection of *Kp* cells from blood and urine samples exhibiting no matrix effects such as luciferase
366 quenching or unspecific increase in background luminescence. While the assay detected *Kp* K64 in
367 urine with the same sensitivity as pure bacterial culture, luminescence peaks retrieved from spiked
368 blood samples indicated a loss of bacterial cells during sample preparation. This was most probably
369 caused by the washing steps during serum collection rather than by blood associated matrix effects as
370 comparable studies have shown that similar optimization steps (serum separation and washing) of
371 spiked blood samples resulted in a 20-50% reduction in bacterial concentration (Moses et al., 2021;
372 Sergueev et al., 2017).

373 The current cutoff for diagnosis of UTIs, one of the most common diseases caused by *Kp,* is $1x10^5$
374 CFUs/ml urine (Becknell et al., 2015). Using our novel reporter phage assay, this minimal pathological
375 *Kp* load can be detected within four hours directly from the patient's urine. Compared to goldstandard
376 methods like PCR, rTUN1::*nLuc* only detects viable *Kp* cells, which can be crucial, e.g., for monitoring
377 therapy success where differentiation between living and dead cells is essential.

378 In addition to that, our approach allows for rapid, real-time assessment of antibiotic resistances (real-
379 time antibiogram) and thus, facilitates treatment of *Kp* K64 infections. Here, susceptibility against
380 therapeutically relevant antibiotics can be tested simultaneously to initial *Kp* detection from clinical
381 samples providing vital information for assessing treatment options in a few hours (depending on the
382 *Kp* load in the sample). In case of an infection with a MDR *Kp* K64 strain with no promising treatment
383 options left, rTUN1::*nLuc* can also function as a companion phage for phage therapy, as positive
384 luminescence readout from reporter phage assays also indicate infectivity of the wildtype TUN1 and
385 thus, qualifies for phage therapy.

386 In conclusion, our results clearly demonstrate the enormous diagnostic capabilities of reporter phages.
387 However, for broad applicability directly from clinical samples, such as urine from patients suffering
388 from UTIs, reporter phages need to be constructed not only for all locally occurring *Kp* K types, but for
389 all clinically relevant pathogens. This would then allow not only the rapid identification of the infection-

390 causing bacterial strain from unknown samples within a few hours, but also the simultaneous
391 generation of a real-time antibiogram of the infection-causing strain as well as the selection of
392 potential candidates for phage therapy.

393 References

394 Acknowledgements

395 We are grateful to Prof. Dr. Ben Moussa from the Military Hospital of Instruction in Tunis, for providing
396 the waste water samples from which we could initially isolate the bacteriophage TUN1, and Daniela
397 Friese for technical assistance.

398 Funding

399 This study was funded by the Medical Biological Defense Research Program of the Bundeswehr
400 Medical Service and supported by supported by the Enable and Enhance Initiative of the federal
401 government of Germany (Ertüchtigungsinitiative der Deutschen Bundesregierung, grant no. OR12-
402 370.43 ERT TUN IMB).

403 Authors' contribution

404 Conceptualization: S.E., J.J.B and P.B.; investigation: R.R., P.B. and S.E.; methodology: S.E. and P.B.;
405 formal analysis and validation: P.B., R.R. and S.E.; visualization: S.E.; writing—original draft
406 preparation: S.E. and P.B.; writing—review and editing: P.B., J.J.B. and S.E.; supervision and project
407 administration: JJ.B. and S.E. All authors have read and agreed to the published version of the
408 manuscript.

409 References

410 Alebachew Woldu, M. (2016). Klebsiella pneumoniae and Its Growing Concern in Healthcare Settings.
411 *Clinical and Experimental Pharmacology*, *06*(01). https://doi.org/10.4172/2161-
412 1459.1000199

413 Anany, H., Brovko, L., El Dougdoug, N. K., Sohar, J., Fenn, H., Alasiri, N., Jabrane, T., Mangin, P.,
414 Monsur Ali, M., Kannan, B., Filipe, C. D. M., & Griffiths, M. W. (2018). Print to detect: A rapid
415 and ultrasensitive phage-based dipstick assay for foodborne pathogens. *Analytical and*
416 *Bioanalytical Chemistry*, *410*(4), 1217–1230. https://doi.org/10.1007/s00216-017-0597-y

417 Babini, G. S., & Livermore, D. M. (2000). Antimicrobial resistance amongst Klebsiella spp. Collected
418 from intensive care units in Southern and Western Europe in 1997–1998. *Journal of*
419 *Antimicrobial Chemotherapy*, *45*(2), 183–189. https://doi.org/10.1093/jac/45.2.183

420 Becknell, B., Schober, M., Korbel, L., & Spencer, J. D. (2015). The diagnosis, evaluation and treatment
421 of acute and recurrent pediatric urinary tract infections. *Expert Review of Anti-Infective*
422 *Therapy*, *13*(1), 81–90. https://doi.org/10.1586/14787210.2015.986097
423 Bhattacharya, S. (2013). Early diagnosis of resistant pathogens: How can it improve antimicrobial
424 treatment? *Virulence*, *4*(2), 172–184. https://doi.org/10.4161/viru.23326
425 Blasco, R., Murphy, M. J., Sanders, M. F., & Squirrell, D. J. (1998). Specific assays for bacteria using
426 phage mediated release of adenylate kinase. *Journal of Applied Microbiology*, *84*(4), 661–
427 666. https://doi.org/10.1046/j.1365-2672.1998.00393.x
428 Borer, A., Saidel-Odes, L., Riesenberg, K., Eskira, S., Peled, N., Nativ, R., Schlaeffer, F., & Sherf, M.
429 (2009). Attributable Mortality Rate for Carbapenem-Resistant *Klebsiella pneumoniae*
430 Bacteremia. *Infection Control & Hospital Epidemiology*, *30*(10), 972–976.
431 https://doi.org/10.1086/605922
432 Casjens, S. R., & Gilcrease, E. B. (2009). Determining DNA packaging strategy by analysis of the
433 termini of the chromosomes in tailed-bacteriophage virions. *Methods in Molecular Biology*
434 *(Clifton, N.J.)*, *502*, 91–111. https://doi.org/10.1007/978-1-60327-565-1_7
435 Chen, J., Alcaine, S. D., Jackson, A. A., Rotello, V. M., & Nugen, S. R. (2017). Development of
436 Engineered Bacteriophages for *Escherichia coli* Detection and High-Throughput Antibiotic
437 Resistance Determination. *ACS Sensors*, *2*(4), 484–489.
438 https://doi.org/10.1021/acssensors.7b00021
439 Chen, J., Picard, R. A., Wang, D., & Nugen, S. R. (2017). Lyophilized Engineered Phages for *Escherichia*
440 *coli* Detection in Food Matrices. *ACS Sensors*, *2*(11), 1573–1577.
441 https://doi.org/10.1021/acssensors.7b00561
442 Davenport, M., Mach, K. E., Shortliffe, L. M. D., Banaei, N., Wang, T.-H., & Liao, J. C. (2017). New and
443 developing diagnostic technologies for urinary tract infections. *Nature Reviews. Urology*,
444 *14*(5), 296–310. https://doi.org/10.1038/nrurol.2017.20

445 Domenico, P., Salo, R. J., Cross, A. S., & Cunha, B. A. (1994). Polysaccharide capsule-mediated
446 resistance to opsonophagocytosis in Klebsiella pneumoniae. *Infection and Immunity*, *62*(10),
447 4495–4499. https://doi.org/10.1128/iai.62.10.4495-4499.1994
448 Eckstein, S., Stender, J., Mzoughi, S., Vogele, K., Kühn, J., Friese, D., Bugert, C., Handrick, S., Ferjani,
449 M., Wölfel, R., Millard, A., Ben Moussa, M., & Bugert, J. J. (2021). Isolation and
450 characterization of lytic phage TUN1 specific for Klebsiella pneumoniae K64 clinical isolates
451 from Tunisia. *BMC Microbiology*, *21*(1), 186. https://doi.org/10.1186/s12866-021-02251-w
452 England, C. G., Ehlerding, E. B., & Cai, W. (2016). NanoLuc: A Small Luciferase Is Brightening Up the
453 Field of Bioluminescence. *Bioconjugate Chemistry*, *27*(5), 1175–1187.
454 https://doi.org/10.1021/acs.bioconjchem.6b00112
455 Garcia, E., Chain, P., Elliott, J. M., Bobrov, A. G., Motin, V. L., Kirillina, O., Lao, V., Calendar, R., &
456 Filippov, A. A. (2008). Molecular characterization of L-413C, a P2-related plague diagnostic
457 bacteriophage. *Virology*, *372*(1), 85–96. https://doi.org/10.1016/j.virol.2007.10.032
458 Goodridge, L., Chen, J., & Griffiths, M. (1999). Development and Characterization of a Fluorescent-
459 Bacteriophage Assay for Detection of *Escherichia coli* O157:H7. *Applied and Environmental*
460 *Microbiology*, *65*(4), 1397–1404. https://doi.org/10.1128/AEM.65.4.1397-1404.1999
461 Grayson, P., Evilevitch, A., Inamdar, M. M., Purohit, P. K., Gelbart, W. M., Knobler, C. M., & Phillips, R.
462 (2006). The effect of genome length on ejection forces in bacteriophage lambda. *Virology*,
463 *348*(2), 430–436. https://doi.org/10.1016/j.virol.2006.01.003
464 Hall, M. P., Unch, J., Binkowski, B. F., Valley, M. P., Butler, B. L., Wood, M. G., Otto, P., Zimmerman,
465 K., Vidugiris, G., Machleidt, T., Robers, M. B., Benink, H. A., Eggers, C. T., Slater, M. R.,
466 Meisenheimer, P. L., Klaubert, D. H., Fan, F., Encell, L. P., & Wood, K. V. (2012). Engineered
467 Luciferase Reporter from a Deep Sea Shrimp Utilizing a Novel Imidazopyrazinone Substrate.
468 *ACS Chemical Biology*, *7*(11), 1848–1857. https://doi.org/10.1021/cb3002478
469 Hartman, L. J., Selby, E. B., Whitehouse, C. A., Coyne, S. R., Jaissle, J. G., Twenhafel, N. A., Burke, R. L.,
470 & Kulesh, D. A. (2009). Rapid real-time PCR assays for detection of Klebsiella pneumoniae
471 with the rmpA or magA genes associated with the hypermucoviscosity phenotype: Screening

472 of nonhuman primates. *The Journal of Molecular Diagnostics: JMD*, *11*(5), 464–471.
473 https://doi.org/10.2353/jmoldx.2009.080136
474 Hennes, K. P., & Simon, M. (1995). Significance of bacteriophages for controlling bacterioplankton
475 growth in a mesotrophic lake. *Applied and Environmental Microbiology*, *61*(1), 333–340.
476 https://doi.org/10.1128/aem.61.1.333-340.1995
477 Herridge, W. P., Shibu, P., O'Shea, J., Brook, T. C., & Hoyles, L. (2020). Bacteriophages of Klebsiella
478 spp., their diversity and potential therapeutic uses. *Journal of Medical Microbiology*, 19.
479 Hinkley, T. C., Singh, S., Garing, S., Le Ny, A.-L. M., Nichols, K. P., Peters, J. E., Talbert, J. N., & Nugen,
480 S. R. (2018). A phage-based assay for the rapid, quantitative, and single CFU visualization of
481 E. coli (ECOR #13) in drinking water. *Scientific Reports*, *8*(1), 14630.
482 https://doi.org/10.1038/s41598-018-33097-4
483 Jain, P., Hartman, T. E., Eisenberg, N., O'Donnell, M. R., Kriakov, J., Govender, K., Makume, M., Thaler,
484 D. S., Hatfull, G. F., Sturm, A. W., Larsen, M. H., Moodley, P., & Jacobs, W. R. (2012). φ^{2}
485 GFP10, a High-Intensity Fluorophage, Enables Detection and Rapid Drug Susceptibility Testing
486 of Mycobacterium tuberculosis Directly from Sputum Samples. *Journal of Clinical*
487 *Microbiology*, *50*(4), 1362–1369. https://doi.org/10.1128/JCM.06192-11
488 Kim, S., Kim, M., & Ryu, S. (2014). Development of an Engineered Bioluminescent Reporter Phage for
489 the Sensitive Detection of Viable *Salmonella* Typhimurium. *Analytical Chemistry*, *86*(12),
490 5858–5864. https://doi.org/10.1021/ac500645c
491 Knothe, H., Shah, P., Krcmery, V., Antal, M., & Mitsuhashi, S. (1983). Transferable resistance to
492 cefotaxime, cefoxitin, cefamandole and cefuroxime in clinical isolates of Klebsiella
493 pneumoniae and Serratia marcescens. *Infection*, *11*(6), 315–317.
494 https://doi.org/10.1007/BF01641355
495 Kollenda, H., Frickmann, H., Helal, R. B., Wiemer, D. F., Naija, H., El Asli, M. S., Egold, M., Bugert, J. J.,
496 Handrick, S., Wölfel, R., Barguellil, F., & Moussa, M. B. (2019). Screening for carbapenemases
497 in ertapenem-resistant *Enterobacteriaceae* collected at a Tunisian hospital between 2014

498 and 2018. *European Journal of Microbiology and Immunology*, *9*(1), 9–13.
499 https://doi.org/10.1556/1886.2018.00033
500 Kurupati, P., Chow, C., Kumarasinghe, G., & Poh, C. L. (2004). Rapid Detection of *Klebsiella*
501 *pneumoniae* from Blood Culture Bottles by Real-Time PCR. *Journal of Clinical Microbiology*,
502 *42*(3), 1337–1340. https://doi.org/10.1128/JCM.42.3.1337-1340.2004
503 Loessner, M. J., Rees, C. E., Stewart, G. S., & Scherer, S. (1996a). Construction of luciferase reporter
504 bacteriophage A511::luxAB for rapid and sensitive detection of viable Listeria cells. *Applied*
505 *and Environmental Microbiology*, *62*(4), 1133–1140. https://doi.org/10.1128/aem.62.4.1133-
506 1140.1996
507 Loessner, M. J., Rees, C. E., Stewart, G. S., & Scherer, S. (1996b). Construction of luciferase reporter
508 bacteriophage A511::luxAB for rapid and sensitive detection of viable Listeria cells. *Applied*
509 *and Environmental Microbiology*, *62*(4), 1133–1140. https://doi.org/10.1128/aem.62.4.1133-
510 1140.1996
511 Matsui, A., Niimi, H., Uchiho, Y., Kawabe, S., Noda, H., & Kitajima, I. (2019). A Rapid ATP
512 Bioluminescence-based Test for Detecting Levofloxacin Resistance Starting from Positive
513 Blood Culture Bottles. *Scientific Reports*, *9*(1), 13565. https://doi.org/10.1038/s41598-019-
514 49358-9
515 McElroy, W. D., & Ballentine, R. (1944). The Mechanics of Bioluminescence. *Proceedings of the*
516 *National Academy of Sciences*, *30*(12), 377–382. https://doi.org/10.1073/pnas.30.12.377
517 Meile, S., Kilcher, S., Loessner, M. J., & Dunne, M. (2020). *Reporter Phage-Based Detection of*
518 *Bacterial Pathogens: Design Guidelines and Recent Developments*. 25.
519 Meile, S., Sarbach, A., Du, J., Schuppler, M., Saez, C., Loessner, M. J., & Kilcher, S. (2020). Engineered
520 Reporter Phages for Rapid Bioluminescence-Based Detection and Differentiation of Viable
521 Listeria Cells. *Applied and Environmental Microbiology*, *86*(11), 14.
522 Merino, S., Camprubí, S., Albertí, S., Benedí, V. J., & Tomás, J. M. (1992). Mechanisms of Klebsiella
523 pneumoniae resistance to complement-mediated killing. *Infection and Immunity*, *60*(6),
524 2529–2535. https://doi.org/10.1128/iai.60.6.2529-2535.1992

525 Moses, S., Vagima, Y., Tidhar, A., Aftalion, M., Mamroud, E., Rotem, S., & Steinberger-Levy, I. (2021).
526 Characterization of Yersinia pestis Phage Lytic Activity in Human Whole Blood for the
527 Selection of Efficient Therapeutic Phages. *Viruses*, *13*(1), 89.
528 https://doi.org/10.3390/v13010089
529 Nakano, R., Nakano, A., Ishii, Y., Ubagai, T., Kikuchi-Ueda, T., Kikuchi, H., Tansho-Nagakawa, S.,
530 Kamoshida, G., Mu, X., & Ono, Y. (2015). Rapid detection of the Klebsiella pneumoniae
531 carbapenemase (KPC) gene by loop-mediated isothermal amplification (LAMP). *Journal of*
532 *Infection and Chemotherapy*, *21*(3), 202–206. https://doi.org/10.1016/j.jiac.2014.11.010
533 Nguyen, C., Makkar, R., Sharp, N. J., Page, M. A., Molineux, I. J., & Schofield, D. A. (2017). Detection of
534 Bacillus anthracis spores from environmental water using bioluminescent reporter phage.
535 *Journal of Applied Microbiology*, *123*(5), 1184–1193. https://doi.org/10.1111/jam.13569
536 Nobrega, F. L., Vlot, M., de Jonge, P. A., Dreesens, L. L., Beaumont, H. J. E., Lavigne, R., Dutilh, B. E., &
537 Brouns, S. J. J. (2018). Targeting mechanisms of tailed bacteriophages. *Nature Reviews*
538 *Microbiology*, *16*(12), 760–773. https://doi.org/10.1038/s41579-018-0070-8
539 Nurmemmedov, E., Castelnovo, M., Catalano, C. E., & Evilevitch, A. (2007). Biophysics of viral
540 infectivity: Matching genome length with capsid size. *Quarterly Reviews of Biophysics*, *40*(4),
541 327–356. https://doi.org/10.1017/S0033583508004666
542 Nurmemmedov, E., Castelnovo, M., Medina, E., Catalano, C. E., & Evilevitch, A. (2012). Challenging
543 Packaging Limits and Infectivity of Phage λ. *Journal of Molecular Biology*, *415*(2), 263–273.
544 https://doi.org/10.1016/j.jmb.2011.11.015
545 Pan, Y.-J., Lin, T.-L., Chen, C.-T., Chen, Y.-Y., Hsieh, P.-F., Hsu, C.-R., Wu, M.-C., & Wang, J.-T. (2015).
546 Genetic analysis of capsular polysaccharide synthesis gene clusters in 79 capsular types of
547 Klebsiella spp. *Scientific Reports*, *5*(1), 15573. https://doi.org/10.1038/srep15573
548 Patel, G., Huprikar, S., Factor, S. H., Jenkins, S. G., & Calfee, D. P. (2008). Outcomes of Carbapenem-
549 Resistant *Klebsiella pneumoniae* Infection and the Impact of Antimicrobial and Adjunctive
550 Therapies. *Infection Control & Hospital Epidemiology*, *29*(12), 1099–1106.
551 https://doi.org/10.1086/592412

552 Pires, D. P., Monteiro, R., Mil-Homens, D., Fialho, A., Lu, T. K., & Azeredo, J. (2021). Designing P.
553 aeruginosa synthetic phages with reduced genomes. *Scientific Reports*, *11*(1), 2164.
554 https://doi.org/10.1038/s41598-021-81580-2
555 Prestinaci, F., Pezzotti, P., & Pantosti, A. (2015). Antimicrobial resistance: A global multifaceted
556 phenomenon. *Pathogens and Global Health*, *109*(7), 309–318.
557 https://doi.org/10.1179/2047773215Y.0000000030
558 Pulkkinen, E. M., Hinkley, T. C., & Nugen, S. R. (2019). Utilizing in vitro DNA assembly to engineer a
559 synthetic T7 Nanoluc reporter phage for Escherichia coli detection. *Integrative Biology:*
560 *Quantitative Biosciences from Nano to Macro*, zyz005. https://doi.org/10.1093/intbio/zyz005
561 Schwaber, M. J., Klarfeld-Lidji, S., Navon-Venezia, S., Schwartz, D., Leavitt, A., & Carmeli, Y. (2008).
562 Predictors of Carbapenem-Resistant *Klebsiella pneumoniae* Acquisition among Hospitalized
563 Adults and Effect of Acquisition on Mortality. *Antimicrobial Agents and Chemotherapy*, *52*(3),
564 1028–1033. https://doi.org/10.1128/AAC.01020-07
565 Sergueev, K., Filippov, A., & Nikolich, M. (2017). Highly Sensitive Bacteriophage-Based Detection of
566 Brucella abortus in Mixed Culture and Spiked Blood. *Viruses*, *9*(6), 144.
567 https://doi.org/10.3390/v9060144
568 Shon, A. S., Bajwa, R. P. S., & Russo, T. A. (2013). Hypervirulent (hypermucoviscous) *Klebsiella*
569 *pneumoniae*: A new and dangerous breed. *Virulence*, *4*(2), 107–118.
570 https://doi.org/10.4161/viru.22718
571 Stewart, L. D., Foddai, A., Elliott, C. T., & Grant, I. R. (2013). Development of a novel phage-mediated
572 immunoassay for the rapid detection of viable *Mycobacterium avium* subsp.
573 *Paratuberculosis*. *Journal of Applied Microbiology*, *115*(3), 808–817.
574 https://doi.org/10.1111/jam.12275
575 Toner, E., Adalja, A., Gronvall, G.K., Cicero, A., Inglesby, T.V. (2015). Antimicrobial resistance is a
576 global health emergency. *Health Secur.* 2015 May-Jun;13(3):153-5. doi:
577 10.1089/hs.2014.0088. PMID: 26042858; PMCID: PMC4486712.
578

579 Turnbull, P.C. (2008) World Health Organization. Anthrax in humans and animals. In: (Editor) PT,
580 editor. Geneva (CH): WHO Press.
581 Zelcbuch, L., Yitzhaki, E., Nissan, O., Gidron, E., Buchshtab, N., Kario, E., Kredo-Russo, S., Zak, N. B., &
582 Bassan, M. (2021). Luminescent Phage-Based Detection of Klebsiella pneumoniae: From
583 Engineering to Diagnostics. *Pharmaceuticals*, *14*(4), 347.
584 https://doi.org/10.3390/ph14040347